Available online at www.sciencedirect.com
SCIENCE DIRECT
Polymer 46 (2005) 12130–12145
polymer
www.elsevier.com/locate/polymer

Electrospinning of hydroxypropyl cellulose fibers and their application in synthesis of nano and submicron tin oxide fibers

Satyajit Shukla, Erik Brinley, Hyoung J. Cho, Sudipta Seal *

Surface Engineering and Nanotechnology Facility (SNF) Lab, Advanced Materials Processing and Analysis Center (AMPAC) and Mechanical Materials Aerospace Engineering (MMAE) Department, University of Central Florida (UCF), Engineering 381, 4000 Central Florida Blvd., Orlando, FL 32816, USA

Received 4 August 2005; received in revised form 6 October 2005; accepted 13 October 2005
Available online 4 November 2005

Abstract

Synthesis of hydroxypropyl cellulose (HPC) fibers via electrospinning has been demonstrated, for the first time, in this investigation. The HPC solution in two different solvents, anhydrous ethanol and 2-propanol, has been utilized with two different tip-to-collector distance (10 and 15 cm) for synthesizing HPC fibers by varying applied voltage within the range of 10–30 kV. It has been shown that, nano (<100 nm) and submicron (>100 nm) HPC fibers can be obtained under the described electrospinning conditions. Average HPC fiber diameter and its bead formation tendency appear to be a function of nature of the solvent and the applied voltage. Characteristic features of electrospinning of HPC fibers appear to be in consonance with the established mechanism of polymer fiber formation via electrospinning. Use of electrospun HPC fibers in synthesizing and depositing highly porous network of nano and submicron tin oxide (SnO_2) fibers on microelectromechanical systems (MEMS) device has been demonstrated.

Keywords: Electrospinning; Hydroxypropyl cellulose; Tin oxide

1. Introduction

Electrospinning is a polymer fiber forming technique that produces fibers of nanometer (<100 nm) to micrometer size in diameters [1–4]. In this process, a polymer solution is placed in a syringe and is subjected to electric fields of several kilovolts. Under the application of electric force, a charged polymer is ejected from the syringe tip and its diameter reduces as it travels towards the grounded substrate, where the deposition of charged polymer fibers takes place. Polymer fibers have been synthesized via electrospinning for different applications, such as wound dressing, drug delivery, catalysts, filtration, composites, membranes, and insecticides [2–5]. It has been now recognized that [3], various electrospinning parameters, such as the type, the molecular weight and the concentration of polymer, the type of solvent, the solution viscosity and the conductivity, the surface tension, the tip-to-collector distance, the applied voltage, the flow rate, and the surrounding atmosphere, are the critical parameters, which significantly affect the characteristics of the electrospun polymer fibers.

In the literature [3], a large variety of polymers have been successfully electrospun into fibers. However, the electrospinning characteristics of the hydroxypropyl cellulose (HPC) polymer have not been investigated in the literature. The HPC polymer has been utilized earlier, as a steric stabilizer, in the synthesis of nanocrystalline ceramic oxide powders [6–8]. However, no attempt has been made to derive the HPC polymer in the fiber form using the electrospinning technique. As a result, the application of fibrous HPC polymer has never been investigated.

In view of this, in the present investigation, we investigate systematically the electrospinning characteristics of the HPC polymer. Moreover, we demonstrate its typical application in deriving the nano and submicron fibers of inorganic materials, typically tin oxide (SnO_2), which is a well known gas sensor.

2. Experimental

2.1. Chemicals

Anhydrous ethanol was purchased from Alfa Aesar (USA) and anhydrous 2-propanol, HPC polymer (molecular weight 80,000 g/mol) and tin(II) chloride ($SnCl_2$) were supplied by

* Corresponding author. Tel.: +1 407 882 1119; fax: +1 407 882 1462.
E-mail addresses: sshukla@ucf.edu (S. Shukla), sseal@mail.ucf.edu (S. Seal).

0032-3861/$ - see front matter © 2005 Elsevier Ltd. All rights reserved.
doi:10.1016/j.polymer.2005.10.070

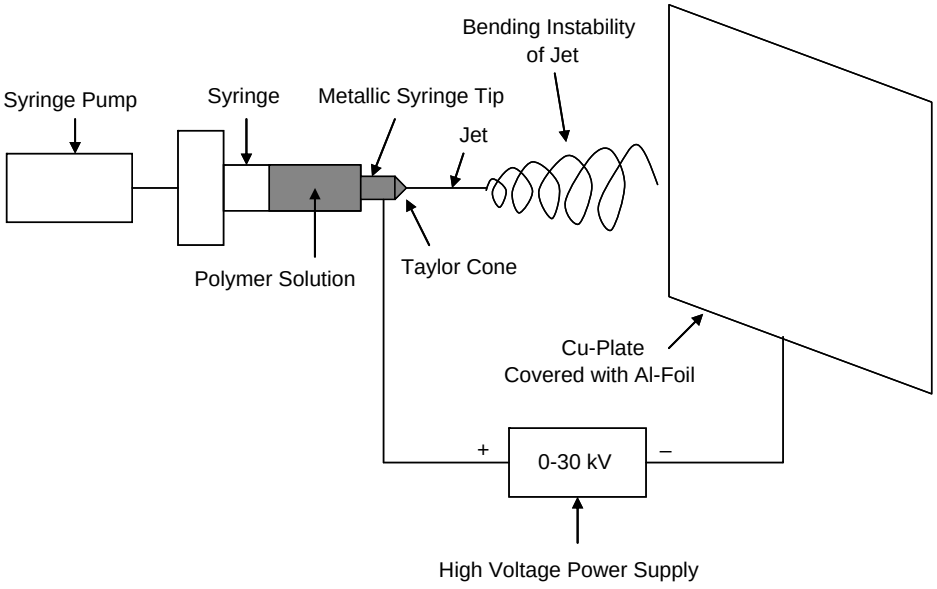

Fig. 1. Schematic representation of the apparatus used for the electrospinning of HPC fibers.

Sigma-Aldrich (USA). All the chemicals were used as received.

2.2. Experimental set-up

The experimental set-up, utilized to obtain the electrospun HPC nano and submicron fibers, is schematically described in Fig. 1. The set-up consists of a syringe (12 mm in diameter, supplied by Fischer Scientific Inc.), syringe pump (New Era Pump Systems Inc., USA), Cu-plate, Al-foil, and a high voltage power supply (0–30 kV, purchased from Glassman Inc., USA). The syringe having a metallic tip holds the viscous polymer solution and is mounted over the syringe pump, which maintains the flow of the polymer solution to the tip of the syringe at a constant rate. The Cu-plate covered with Al-foil is placed in front of the syringe tip to collect the electrospun nano and submicron HPC fibers by adjusting the tip-to-collector distance as desired. The positive terminal of the high voltage power supply (0–30 kV) is connected to the metallic syringe-tip while the negative (ground) terminal is connected to the Cu-plate covered with Al foil.

2.3. Electrospinning of HPC polymer

Proper amount of the HPC polymer (15 wt%) was first weighed and dissolved completely in the appropriate solvent under continuous stirring using the magnetic stirrer (note: the amount of HPC polymer to be dissolved is calculated with respect to the initial weight of the alcohol (pure solvent) and not with respect to the total weight of the final polymer solution). The beaker containing the HPC solution was covered with a paraffin tape during stirring. Proper amount of HPC solution was then taken in the syringe, which was then placed on the syringe pump. After applying the desired electric potential in between the metallic syringe-tip and the Cu-plate, the HPC solution was continuously fed to the syringe-tip at the constant flow rate of 20 μl/min using the syringe pump. Depending on the electrospinning conditions, the drop of the HPC solution coming out of the syringe-tip was noted to form a conical shape, from which a jet of HPC solution was observed to emerge. The actual deposition of the nano and submicron HPC fibers, however, could not be viewed by naked eye. However, the Al-foil gradually changed its color from grey to white during the electrospinning experiments.

The electrospinning of the HPC polymer dissolved in anhydrous ethanol was first conducted for the two different tip-to-collector distances, 10 and 15 cm, by increasing the applied voltage within the range of 10–30 and 15–30 kV, respectively, in steps of 5 kV. The minimum applied voltage for each tip-to-collector distance was calculated by using the minimum electric field strength value of 1 kV/cm. The above electrospinning procedure was then repeated for the HPC polymer dissolved in anhydrous 2-propanol. Unless otherwise stated, all the electrospinning experiments reported in this investigation are conducted for 30 min.

2.4. Electrospinning of HPC polymer with Sn-precursor

These experiments were specifically designed to obtain the nano and submicron semiconductor SnO_2 fibers using the electrospun HPC fibers as templates. For this purpose, 0.45 M of $SnCl_2$ was dissolved completely in the previously prepared 15 wt% HPC solution in ethanol with the HPC to $SnCl_2$ weight ratio of 1.75, which yielded 36 wt% salt content within the HPC fibers prior to the calcinations (note: the amount of $SnCl_2$ to be dissolved is calculated with respect to the initial weight of the alcohol (pure solvent)). The tip-to-collector distance of 10 cm was selected with the applied potential difference of 15 kV. A MEMS device, having four interdigitated Au electrode configurations (note: the preparation of the MEMS

device for gas sensor application has been already described in detail elsewhere [9]) was used as a substrate for the deposition of the nano and submicron HPC fibers containing Sn-Precursor. Before the electrospinning experiments, the surface of the MEMS device was masked using a double sided tape; however, an opening was kept in the center where the four interdigitated Au electrodes were located. After the electrospinning of the HPC fibers with Sn-precursor, the tape was removed and the MEMS device was subjected to thermal treatment at 400 °C using the heating rate of 30 °C/min and the holding time of 1 h. The device was then cooled down to room temperature inside the furnace.

2.5. Characterization

The surface chemistry of the electrospun HPC and SnO_2 fibers were studied using the X-ray photoelectron spectroscopy (XPS) by utilizing PHI ESCA spectrometer (model 5400, Perkin–Elmer, Minnesota), having the energy resolution of $\pm$ 0.1 eV, at a base pressure of 5×10^{-9} Torr using Mg Kα radiation (1253.6 eV). The X-ray power during the analysis was either 250 W (for HPC fibers) or 350 W (for SnO_2 fibers). Both the survey and the high-resolution narrow-scan spectra were recorded at the pass energies of 44.75 and 35.75 eV, respectively, to achieve the maximum spectral resolution. The binding energy (BE) of the Au $4f_{7/2}$ at 84.0 ± 0.1 eV was used to calibrate the BE scale of the spectrometer. Any charging shifts produced by the samples were carefully corrected either using the C(1s) BE of 284.6 eV in the adventitious carbon [10] or that of the C–H bond, 285.0 eV, within the HPC polymer [7].

The morphology and the average diameter of the electrospun HPC and SnO_2 fibers were analyzed using the scanning electron microscopy (SEM) (JSM-6400F, JEOL, Tokyo, Japan). To avoid any surface charging during the SEM analysis, the electrospun HPC fiber mat (collected on the Al foil) and the MEMS device (with SnO_2 fibers) were coated with approximately 30 nm Au–Pd layer using a sputter coater (K350, Emitech, Ashford, Kent, England).

3. Results

3.1. Electrospinning of HPC polymer in ethanol

3.1.1. Tip-to-collector distance of 10 cm

Typical SEM images of HPC fibers as a function of applied voltage, electrospun with the tip-to-collector distance of 10 cm using the HPC solution in ethanol, are presented in Figs. 2 and 3 at low and high magnifications, respectively. It is noted that, HPC fibers are successfully obtained under these electrospinning conditions. In Fig. 2, beads are observed with the HPC fibers, showing a typical 'bead-on-string' morphology under all processing conditions. Very fine beads are observed at low applied potential difference of 10 kV (electric field strength of 1 kV/cm), Fig. 2(a). With increasing applied voltage above 10 kV, the number of beads and the average bead size are qualitatively observed to increase, Figs. 2(a)–(d). However, at the highest applied voltage of 30 kV, Fig. 2(e), although more number of beads is formed, the average bead size is noted to decrease suddenly. Moreover, under all processing conditions, it is observed that, the HPC fibers are arranged in a fashion, which gives rise to highly porous morphology of the deposited non-woven fiber mat.

The effect of applied potential difference on the HPC fiber diameter is qualitatively observed in Fig. 3. The variation in the minimum and the maximum HPC fiber diameters measured as a function of applied voltage is plotted in Fig. 4(a) (note: in Fig. 4, the variation in the minimum and the maximum HPC fiber diameters as a function of applied voltage, obtained under all processing conditions, is plotted). In Fig. 3(a), which corresponds to the lowest applied voltage of 10 kV (electric field strength of 1 kV/cm), the minimum and the maximum fiber diameters are observed to be 80 and 300 nm, respectively, Fig. 4(a). Thus, both nano as well as submicron HPC fibers are formed under these electrospinning conditions. Interestingly, the very fine HPC fibers tend to break due to an exposure to the electron beam, Fig. 3(a), during the SEM analysis. With increasing applied potential difference, the number of fine broken fibers is observed to decrease, Figs. 3(a)–(c), and the maximum HPC fiber diameter is simultaneously observed to increase, Fig. 4(a). Above 20 kV, however, fine broken HPC fibers are formed again, Figs. 3(d) and (e); while the maximum HPC fiber diameter is observed to decrease suddenly at the applied voltage of 30 kV, Fig. 4(a). Moreover, in Fig. 3, the average inter fiber spacing is qualitatively noted increase with the applied voltage; however, it decreases suddenly at the highest applied potential difference of 30 kV. Under almost all processing conditions, the formation of 'branched fibers' is clearly evident in Fig. 3.

3.1.2. Tip-to-collector distance of 15 cm

Typical SEM images of HPC fibers as a function of applied voltage, electrospun with the tip-to-collector distance of 15 cm using the HPC solution in ethanol, are presented in Figs. 5 and 6 at low and high magnifications, respectively. It is noted that, the nano and submicron HPC fibers are successfully obtained under these electrospinning conditions as well. Similar to the previous case, typical 'bead-on-string' morphology is observed under all processing conditions, Fig. 5. Small size beads are again observed at the lowest applied potential difference of 15 kV (electric field strength of 1 kV/cm), Fig. 5(a). The number of beads and the average bead size are qualitatively observed to increase with increasing applied potential difference within the range of 15–30 kV. However, in contrast to the previous case, at the applied voltage of 30 kV, Fig. 5(d), no sudden decrease in the average bead size is noted. Overall, it appears that, for the tip-to-collector distance of 15 cm, the characteristics of the bead formation are more or less similar to the previous case; nevertheless, the applied voltages greater than 30 kV may be required to cause the decrease in the average bead size.

The variation in the average HPC fiber diameter and its size distribution as a function of the applied potential difference, for

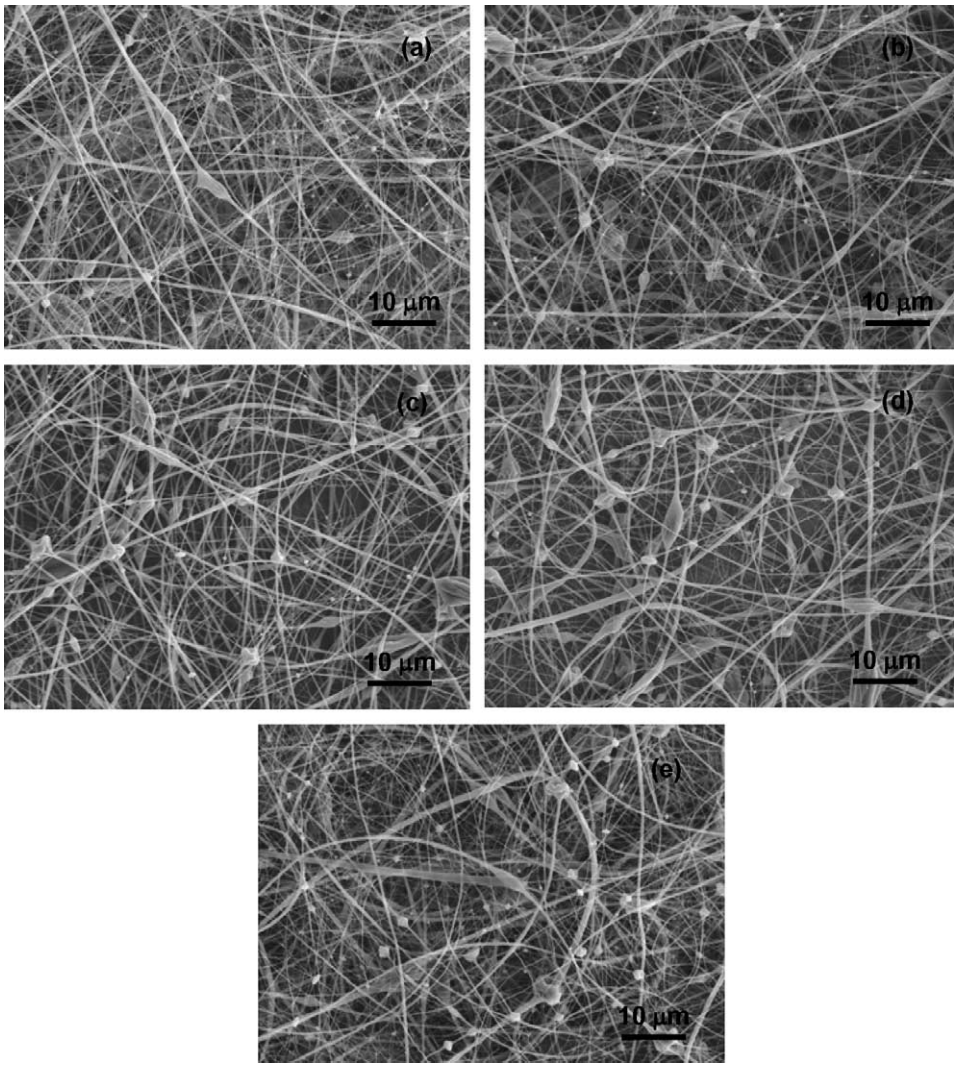

Fig. 2. SEM images, at low magnification, showing the nano and submicron HPC fibers, as a function of applied voltage, electrospun by using 15 wt% HPC solution in anhydrous ethanol and tip-to-collector distance of 10 cm. (a) 10 kV, (b) 15 kV, (c) 20 kV, (d) 25 kV, and (e) 30 kV.

the tip-to-collector distance of 15 cm, can be qualitatively observed in Fig. 6. The variation in the minimum and the maximum HPC fiber diameters as a function of applied voltage, measured under these electrospinning conditions, is plotted in Fig. 4(b). In Fig. 6(a), which corresponds to the lowest applied voltage of 15 kV (electric filed strength of 1 kV/cm), the minimum and the maximum HPC fiber diameters of 80 and 500 nm are observed, respectively. Thus, nano and submicron HPC fibers are formed under these electrospinning conditions as well. Similar to the tip-to-collector distance of 10 cm, Fig. 3(a), very fine HPC fibers are seen at the lowest applied voltage of 15 kV, Fig. 6(a), which tend to break under the electron beam during the SEM analysis. With increasing applied potential difference, the average HPC fiber diameter is observed to increase, Fig. 6(b), with the simultaneous and almost complete elimination of the fine broken fibers. Smooth, straight, and continuous HPC fibers are clearly seen to form under these electrospinning conditions. With the increasing applied voltage, Fig. 6(c), the average HPC fiber diameter is qualitatively noted to increase further. Although, the 'branched fibers' are formed under almost all electrospinning conditions, their number density is much larger at the applied voltage of 25 kV, Fig. 6(c). Very few fine broken fibers are present at some locations in Fig. 6(c). Similar to the observation made for the tip-to-collector distance of 10 cm, Fig. 3(e), the average HPC fiber diameter is qualitatively noted to decrease suddenly at the applied voltage of 30 kV, Fig. 6(d), due to the formation of more number of fine HPC fibers. The maximum HPC fiber diameter measured is, however, noted to increase continuously with the applied voltage, Fig. 4(b). Comparison of Figs. 4(a) and (b) shows that, the variation in the maximum HPC fiber diameter as a function of the applied voltage for the tip-to-collector distance of 15 cm, Fig. 4(b), is shifted to the right hand side relative to that observed for the tip-to-collector distance of 10 cm, Fig. 4(a). Similarly, the average inter fiber spacing is also observed to increase with increasing applied voltage, Figs. 6(a)–(c), and then to decrease suddenly at the highest applied potential difference of 30 kV, Fig. 6(d).

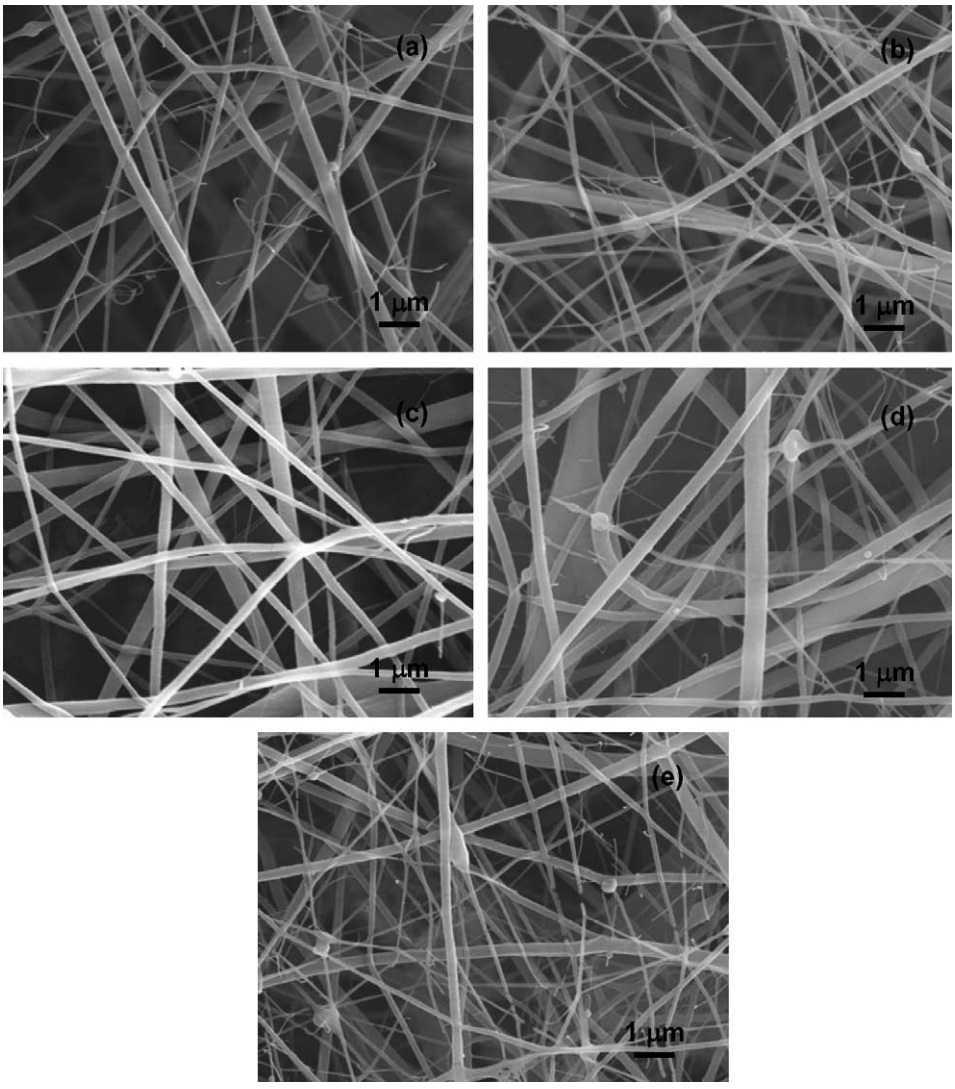

Fig. 3. SEM images, at high magnification, showing the nano and submicron HPC fibers, as a function of applied voltage, electrospun by using 15 wt% HPC solution in anhydrous ethanol and tip-to-collector distance of 10 cm. (a) 10 kV, (b) 15 kV, (c) 20 kV, (d) 25 kV, and (e) 30 kV.

3.2. Electrospinning of HPC polymer in 2-propanol

3.2.1. Tip-to-collector distance of 10 cm

Typical SEM images of HPC fibers as a function of applied potential difference, electrospun with the tip-to-collector distance of 10 cm using the HPC solution in 2-propanol, are presented in Figs. 7 and 8 at low and high magnifications, respectively. The HPC fibers are, thus, successfully formed using 2-propanol as a solvent. Comparison of Figs. 2 and 7 indicates that, almost no beads are observed under all electrospinning conditions when the HPC fibers are formed using 2-propanol as a solvent instead of ethanol.

The variation in the HPC fiber diameter and its average size distribution as a function of applied voltage is qualitatively noted in Fig. 8. The variation in the minimum and the maximum HPC fiber diameters as a function of applied voltage, measured using these images, is plotted in Fig. 4(a). For the lowest applied voltage of 10 kV (electric field strength of 1 kV/cm), Fig. 8(a), the minimum and the maximum fiber diameters of 150 and 750 nm are observed, respectively, which are larger than those observed with ethanol solvent (80 and 300 nm, respectively) under similar electrospinning conditions, Fig. 3(a). In Fig. 8(a), fine broken HPC fibers are also observed; however, there number density is lesser than that observed in Fig. 3(a). With increasing applied voltage, the average HPC fiber diameter is qualitatively observed to increase, Figs. 8(b) and (c), with the corresponding increase in the minimum and the maximum HPC fiber diameters, Fig. 4(a). Comparison of Fig. 8(b) with Fig. 3(b) and Fig. 8(c) with Fig. 3(c) suggests that, even at higher applied voltages, the HPC fibers with larger average diameter are formed when 2-propanol, instead of ethanol, is used as a solvent. Interestingly, with further increase in the applied voltage, Figs. 8(d) and (e), the average HPC fiber diameter is qualitatively noted to decrease with the corresponding decrease in the minimum and maximum HPC

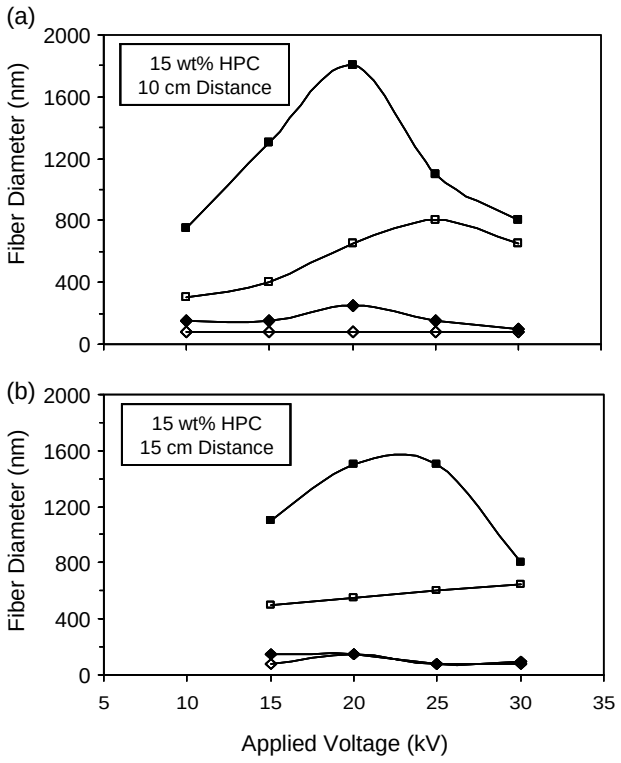

Fig. 4. Variation in the minimum (♦, ◇) and the maximum (■, □) HPC fiber diameter as a function of applied voltage obtained under different electrospinning conditions. Solid and open data points represent 15 wt% HPC solutions in 2-propnaol and ethanol solvents, respectively.

fiber diameters above the applied voltage of 20 kV, Fig. 4(a). It is noted that, the variation in the maximum HPC fiber diameter as a function of applied potential difference is shifted to the right hand side for ethanol than that observed for 2-propanol. Moreover, the tendency to form the fine HPC fibers at the highest applied voltage of 30 kV is observed to be less with 2-propanol, Fig. 8(e), than that observed with ethanol, Fig. 3(e). In Fig. 8, the average inter fiber spacing is observed to increase first with the applied voltage, Figs. 8(a)–(c); however, it decreases with further increase in the applied potential difference above 20 kV, Figs. 8(d)–(e).

3.2.2. Tip-to-collector distance of 15 cm

Typical SEM images of HPC fibers as a function of applied potential difference, electrospun with the tip-to-collector distance of 15 cm using the HPC solution in 2-propanol, are presented in Figs. 9 and 10 at low and high magnifications, respectively. The HPC fibers are successfully obtained using 2-propanol as a solvent with the working distance of 15 cm. Under these electrospinning conditions, the comparison of Figs. 5 and 9 indicates that, no beads are observed when the HPC fibers are formed using 2-propanol as a solvent. Thus, the bead formation has been successfully eliminated by changing the solvent from ethanol to 2-propanol for both the working distances of 10 and 15 cm.

The variation in the HPC fiber diameter and its average size distribution as a function of applied potential difference, for the working distance of 15 cm, is qualitatively observed in Fig. 10. The corresponding variation in the minimum and the

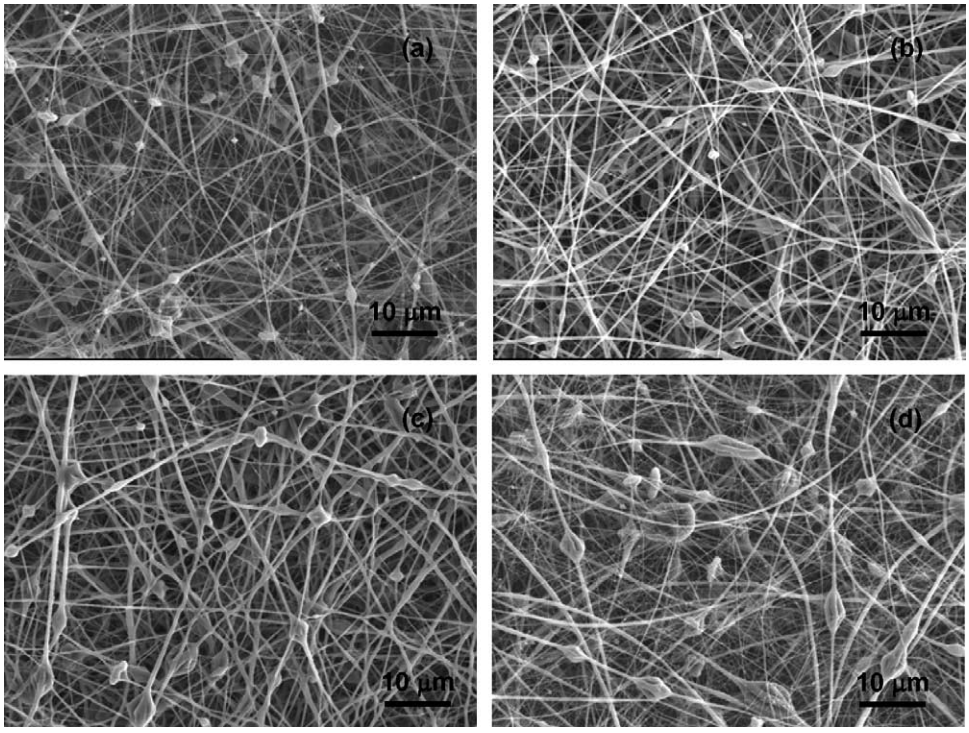

Fig. 5. SEM images, at low magnification, showing the nano and submicron HPC fibers, as a function of applied voltage, electrospun by using 15 wt% HPC solution in anhydrous ethanol and tip-to-collector distance of 15 cm. (a) 15 kV, (b) 20 kV, (c) 25 kV, and (d) 30 kV.

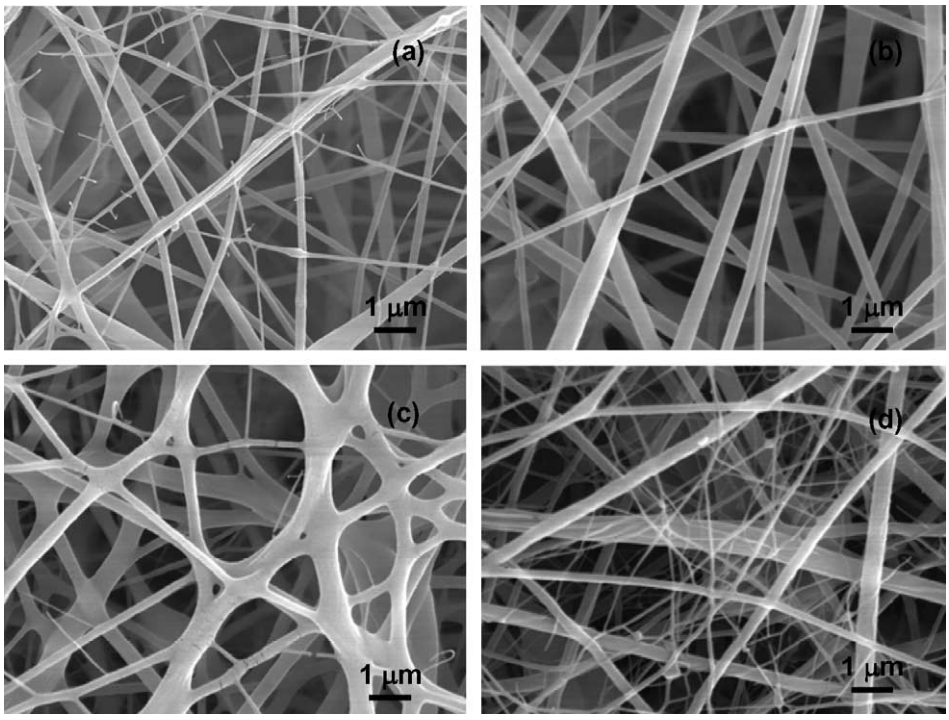

Fig. 6. SEM images, at high magnification, showing the nano and submicron HPC fibers, as a function of applied voltage, electrospun by using 15 wt% HPC solution in anhydrous ethanol and tip-to-collector distance of 15 cm. (a) 15 kV, (b) 20 kV, (c) 25 kV, and (d) 30 kV.

maximum HPC fiber diameters as a function of applied voltage, measured using these images, is plotted in Fig. 4(b). For the lowest applied voltage of 15 kV (electric field strength of 1 kV/cm), Fig. 10(a), the minimum and the maximum HPC fiber diameters are observed to be 150 and 1000 nm, respectively, which are larger than those observed with ethanol solvent (80 and 500 nm, respectively) under similar electrospinning conditions, Fig. 6(a). In Figs. 9(a) and 10(a), no fine broken HPC fibers are observed. With increasing applied potential difference, the maximum (Fig. 4(b)) and the average (Fig. 10(b)) HPC fiber diameters, are noted to increase first and then to decrease (Figs. 10(c) and (d)) with increasing applied voltage above 20 kV. Similar to the observation made with ethanol, Fig. 4(a), the variation in the maximum HPC fiber diameter as a function of applied voltage, for the HPC solution in 2-propanol, Fig. 4(b), is shifted to the right hand side with increasing tip-to-collector distance. In Fig. 10, an increased number of 'branched fibers' is typically noted at higher applied voltages. Thus, the 'branched fibers' are observed for the HPC solutions in both ethanol and 2-propanol. As in the previous case, the decrease in the average inter fiber spacing at higher applied potential differences (above 20 kV) is also evident in Fig. 10.

3.3. SnO_2 fibers synthesized using electrospun HPC fibers as templates

3.3.1. Morphological analysis

Typical SEM images of the HPC fibers electrospun by dissolving $SnCl_2$ using ethanol as solvent (other processing conditions are given in the figure caption) are presented in Fig. 11. It is clear that, the HPC polymer can be electrospun along with the dissolved Sn^{2+} and Cl^- ions. Very fine beads in small number are observed with typical 'bead-on-string' morphology in Fig. 11(a). Comparison of Fig. 2(b) with Fig. 11(a) reveals that, the average bead size decreases with the addition of Sn^{2+} and Cl^- ions into the HPC polymer solution. On the other hand, by comparing Fig. 3(b) with Fig. 11(b), it is noted that, both the average HPC fiber size and the average inter fiber distance increase with the addition of Sn^{2+} and Cl^- ions to the HPC solution. The minimum and the maximum HPC fiber diameters of 90 and 720 nm are measured, respectively, using Fig. 11(b), which are larger than those (80 and 400 nm, respectively) measured without the addition of Sn^{2+} and Cl^- ions under similar electrospinning conditions, Fig. 4(a).

Typical SEM images of SnO_2 fibers, deposited on the MEMS device by calcining the as deposited HPC fibers containing Sn^{2+} and Cl^- ions, are presented in Fig. 12. The MEMS device with four interdigitated Au electrode configurations is shown in Fig. 12(a) along with the highly porous network of SnO_2 fibers. In Fig. 12(b), two Au electrodes with the electrode distance of 50 μm are seen, which are short circuited by the SnO_2 fibers. The SnO_2 fiber size can be estimated using the SEM image obtained at high magnification, Fig. 12(c), and is measured to be within the range of 45–280 nm. This size range of SnO_2 fibers is lesser than that (90–720 nm) of the HPC fibers containing the Sn^{2+} and Cl^- ions, Fig. 11(c), which possibly suggests the shrinkage of the deposited fibers due to the decomposition of the HPC

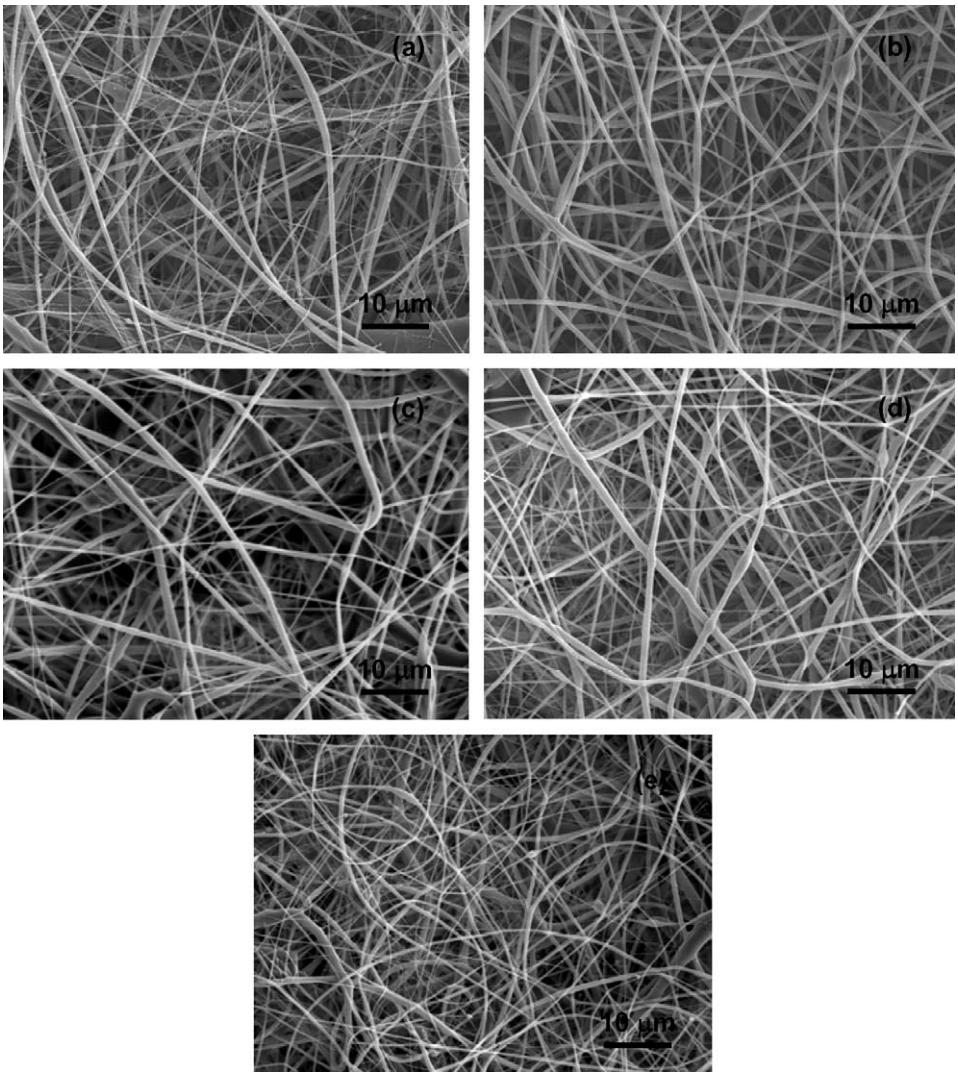

Fig. 7. SEM images, at low magnification, showing the nano and submicron HPC fibers, as a function of applied voltage, electrospun by using 15 wt% HPC solution in anhydrous 2-propanol and tip-to-collector distance of 10 cm. (a) 10 kV, (b) 15 kV, (c) 20 kV, (d) 25 kV, and (e) 30 kV.

polymer at the calcination temperature. The MEMS device with the deposited nano and submicron SnO_2 fibers exhibits the average electrical resistance of 450 Ω as measured using the multimeter, which further suggests the semiconductor nature of nano and submicron SnO_2 fibers.

3.3.2. Bulk chemical analysis

Typical EDX analysis of the HPC fibers obtained under different electrospinning conditions are presented in Fig. 13. The EDX spectra of HPC fibers electrospun with 10 cm tip-to-collector distance and applied voltage of 15 kV is presented in Fig. 13(a). Only C and O peaks are identified under these electrospinning conditions. Particularly, an intense C is peak is noted, which strongly indicates the presence of the HPC polymer. The Au and Pd peaks have been originated from the sputtering process utilized to avoid the charging effects during the image analysis. Due to the relatively larger HPC fibers mat thickness and smaller inter fiber spacing, no peak from the Al foil (substrate) is noted in Fig. 13(a).

The EDX spectrum obtained from the HPC fibers electrospun with the addition of Sn^{2+} and Cl^- ions is shown in Fig. 13(b). Correspondingly, the additional peaks from Sn and Cl are identified in Fig. 13(b) along with the Al peak from the substrate. The presence of Al peak from the substrate is possibly due to an increased inter fiber spacing associated with the addition of Sn^{2+} and Cl^- ions to the HPC polymer solution (compare Figs. 3(b) and 11(b)). Very intense C peak is again noted in this spectrum as well.

The EDX spectrum obtained after the calcination treatment of HPC fibers, containing the Sn^{2+} and Cl^- ions, deposited on the MEMS device is presented in Fig. 13(c). Comparison of Fig. 13(b) with Fig. 13(c) reveals that, the calcination treatment results in a drastic reduction in the intensity of the C peak possibly due to the degradation of the HPC polymer at the calcination temperature. Moreover, the Cl peak also vanishes due to the calcination treatment; while, the Sn peak becomes relatively more intense. The Si peak noted in Fig. 13(c) is from the MEMS device, which is used as the substrate for the deposition of the fibrous SnO_2.

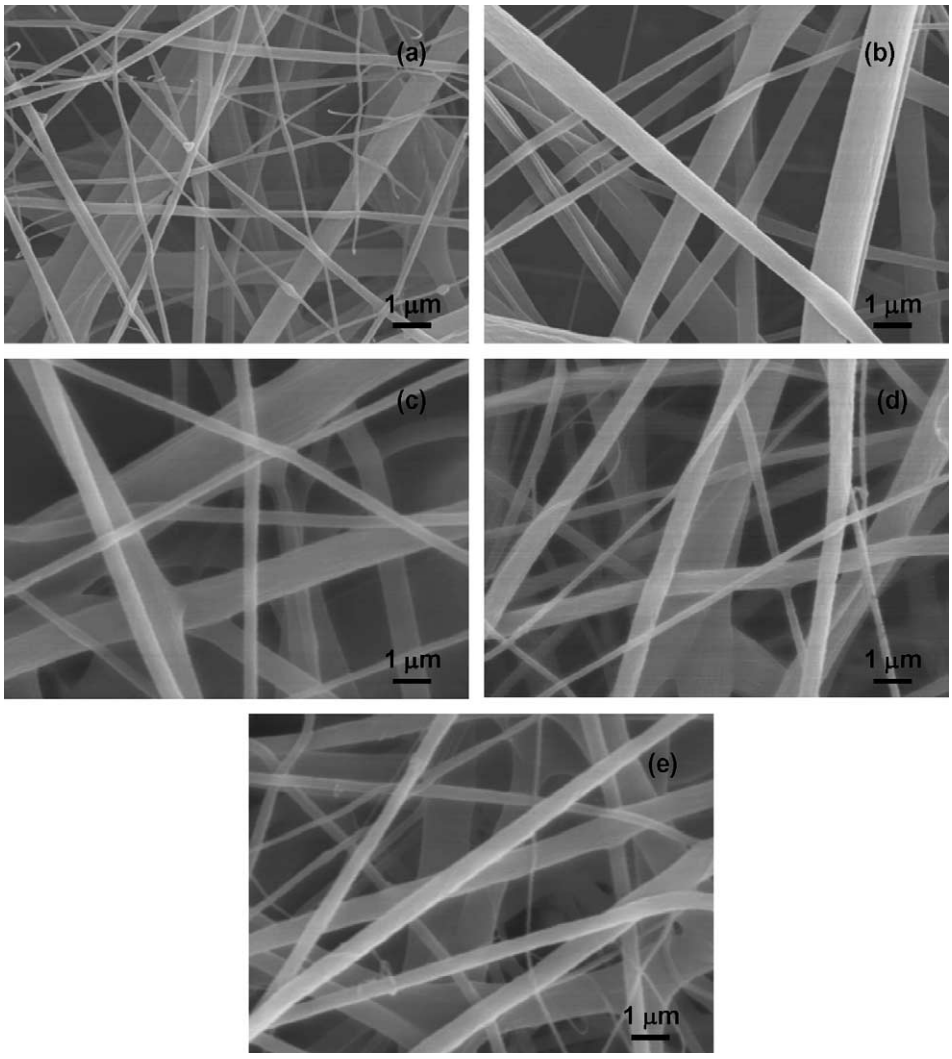

Fig. 8. SEM images, at high magnification, showing the nano and submicron HPC fibers, as a function of applied voltage, electrospun by using 15 wt% HPC solution in anhydrous 2-propanol and tip-to-collector distance of 10 cm. (a) 10 kV, (b) 15 kV, (c) 20 kV, (d) 25 kV, and (e) 30 kV.

3.3.3. Surface chemical analysis

Typical XPS broad scan spectra for the HPC and SnO_2 fibers, obtained under different electrospinning conditions, are presented in Fig. 14. In Fig. 14(a), the XPS broad scan of the HPC fibers is shown, which shows the C and O species on the fiber surface. The broad scan analysis for the HPC fibers electrospun with the Sn^{2+} and Cl^- ions, Fig. 14(b), reveals the additional presence of Sn and Cl species on the fiber surface. In contrast to the bulk analysis, Fig. 13(c), small amount of residual Cl is still noted on the fiber surface after the calcination treatment at higher temperature, Fig. 14(c).

Typical narrow scan spectra obtained for the C(1s), Sn(3d), and Cl(2p), within the BE ranges of 280–295, 480–505, and 192–207 eV, are presented in Figs. 15–17, respectively for different electrospinning conditions. The deconvolution of the C(1s) spectra corresponding to the HPC fibers, electrospun without and with Sn^{2+} and Cl^- ions, reveals the presence of three sub-peaks located at the BE positions 285.0, 286.9, and 287.9 eV, Fig. 15(a), and 285.0, 287.3, and 289.1 eV, Fig. 15(b), respectively. These three sub-peaks are related to the C–H, C–O–H/C–O–C, and C=O bond within the HPC polymer, respectively [7]. Comparison of Figs. 15(a) and (b) shows that, in the presence of Sn^{2+} and Cl^- ions, the BE positions of C–O–H/C–O–C and C=O peaks are shifted to higher BE values with decrease in the intensity of the C–O–H/C–O–C peak. Further, the deconvolution of the C(1s) spectrum, Fig. 15(c), corresponding to the SnO_2 fibers (obtained after the calcinations treatment of the HPC fibers containing Sn^{2+} and Cl^- ions) reveals the presence of four peaks in contrast to the three peaks detected earlier. The additional intense peak, detected at the BE position of 284.6 eV, has been attributed the adventitious C–H bond [10]. The C–H, C–O–H/C–O–C, and C=O peaks corresponding to the HPC polymer are observed at 285.0, 286.2, and 287.6 eV, respectively. Thus, although the bulk C is removed via calcination treatment, Fig. 13(c), some trace amount of the HPC polymer is still retained on the surface of the SnO_2 fibers.

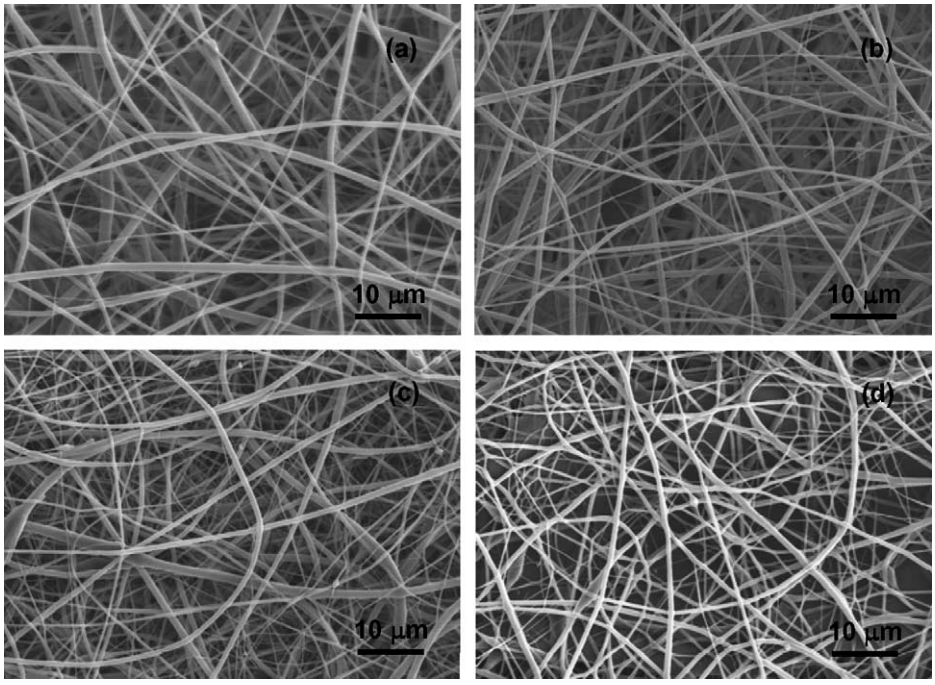

Fig. 9. SEM images, at low magnification, showing the nano and submicron HPC fibers, as a function of applied voltage, electrospun by using 15 wt% HPC solution in anhydrous 2-propanol and tip-to-collector distance of 15 cm. (a) 15 kV, (b) 20 kV, (c) 25 kV, and (d) 30 kV.

In Figs. 16(a) and (b), Sn $3d_{5/2}$ BE levels of 490.2 and 487.0 eV, and in Figs. 17(a) and (b), the Cl $2p_{3/2}$ BE levels of 201.1 and 198.2 eV have been noted for the Sn and Cl species, respectively, which are present on the surface of the HPC fibers (obtained before the calcination treatment) and the SnO_2 fibers (obtained after the calcination treatment). Higher Sn $3d_{5/2}$ and Cl $2p_{3/2}$ BE values are noted when the Sn and Cl species are present within the electrospun HPC fibers. However, their BE values reduce significantly, by almost the same amount, after the calcination treatment, which effectively burns the HPC polymer. These shifts in the Sn $3d_{5/2}$ and Cl $2p_{3/2}$ BE values suggest the possible interaction of the Sn^{2+} and Cl^{-} ions with

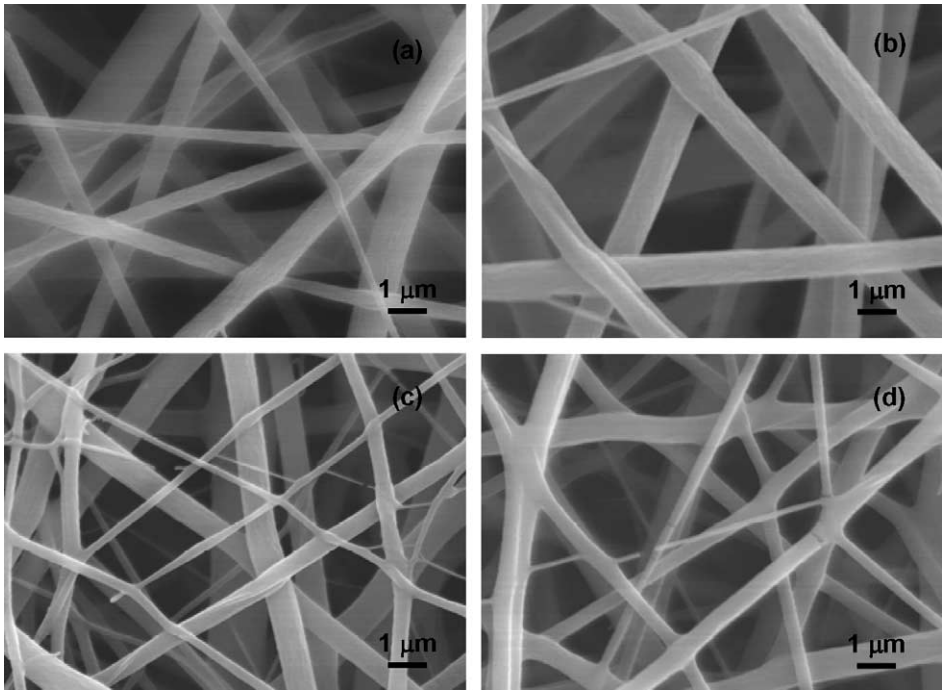

Fig. 10. SEM images, at high magnification, showing the nano and submicron HPC fibers, as a function of applied voltage, electrospun by using 15 wt% HPC solution in anhydrous 2-propanol and tip-to-collector distance of 15 cm. (a) 15 kV, (b) 20 kV, (c) 25 kV, and (d) 30 kV.

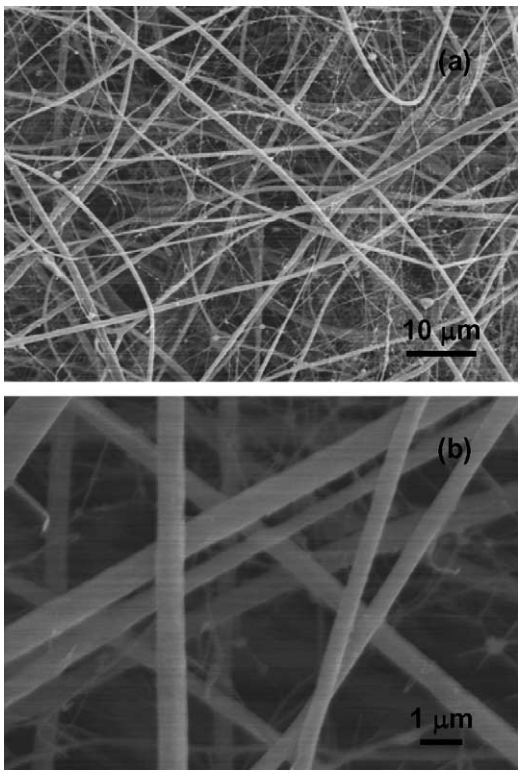

Fig. 11. SEM images, at low (a) and high (b) magnifications, showing the nano and submicron HPC fibers, electrospun by dissolving the Sn^{2+} and Cl^{-} ions into 15 wt% HPC solution in anhydrous ethanol. Electrospinning conditions are: tip-to-collector distance = 10 cm and applied voltage = 15 kV.

the HPC polymer. The Sn $3d_{5/2}$ BE of 487.0 eV obtained after the calcination treatment, further suggests the presence of Sn^{4+} specie, indicating the formation of nano and submicron fibers of SnO_2 [9].

4. Discussion

In the present investigation, electrospinning technique has been successfully utilized to synthesize nano and submicron HPC fibers. Two different solvents (anhydrous ethanol and 2-propanol) and two different tip-to-collector distances (10 and 15 cm) have been used for this purpose; while, the applied potential difference has been varied within the range of 10–30 kV (with the minimum electric filed strength of 1 kV/cm) with the HPC polymer concentration being kept constant at 15 wt%. Various characteristics of electrospinning of HPC fibers have been observed and are explained in the following discussion by considering the established mechanism of polymer fiber formation via electrospinning process [1–3]. Hence, we first briefly review the mechanism of polymer fiber formation via electrospinning, which basically involves stretching, drying, and solidifying the electrical instability [11–16] of the electrospun fluid jet.

4.1. Mechanism of polymer fiber formation via electrospinning

The polymer solution held in the syringe tends to form a droplet with flat surface and is held at the syringe tip by the surface tension force. When the high voltage is applied to the polymer solution in the syringe, the droplet surface is pulled into the approximate shape of a section of a sphere by the electric forces and the surface tension. As the bulge forms, the charges move through the polymer solution to concentrate in the area that is protruding most. The accumulation of the electric charges causes the droplet surface to protrude more, and since the charge per unit surface area is the highest near the greatest protrusion, the surface is pulled further into a conical shape, which is known as a Taylor cone. The charge per unit surface area at the tip of the cone increases as the radius near the tip of the cone decreases. As the applied potential difference is increased, a jet of charged polymer solution is pulled from the Taylor cone and the electrospinning process begins.

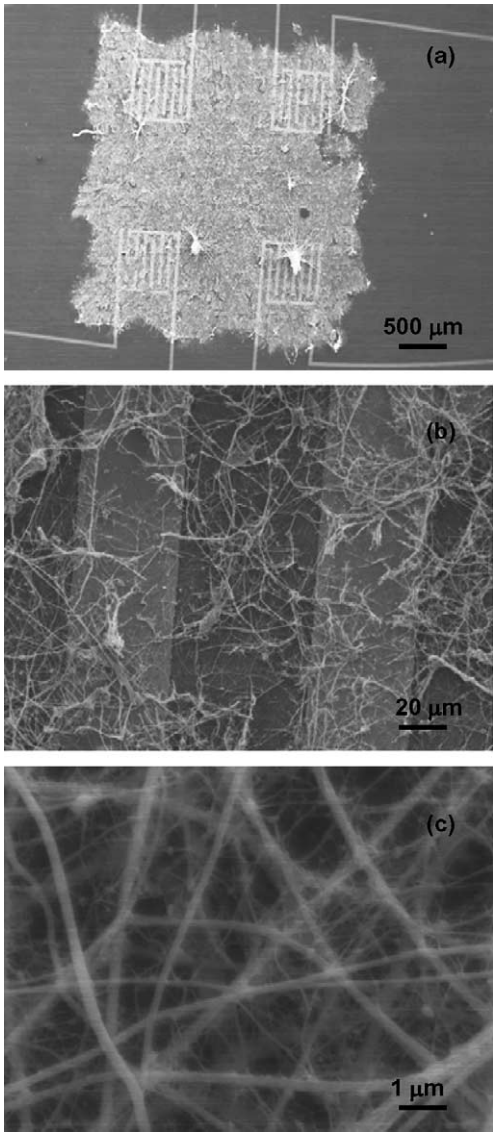

Fig. 12. SEM images (a)–(c), at different magnifications, showing the nano and submicron SnO_2 fibers deposited on the MEMS device, obtained after calcining the HPC fibers, containing Sn^{2+} and Cl^{-} ions, at 400 °C. Electrospinning conditions are: tip-to-collector distance = 10 cm and applied voltage = 15 kV. Four interdigitated electrode configurations are visible in (a). In (b), two Au electrodes with 50 μm spacing are seen.

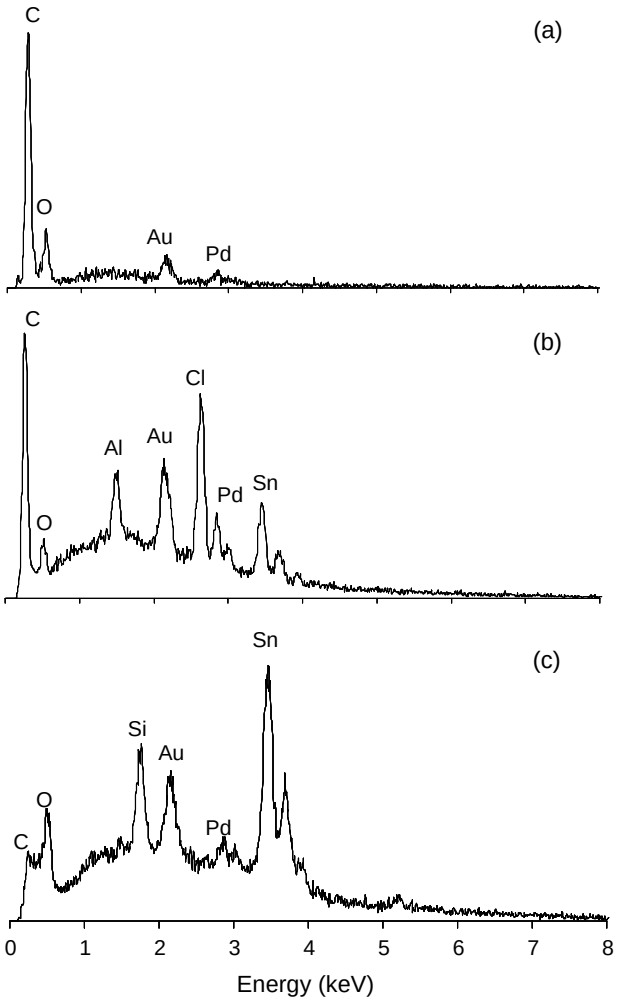

Fig. 13. EDX analysis of HPC fibers without (a) and with (b) Sn^{2+} and Cl^{-} ions, and SnO_2 fibers deposited on the MEMS device (c). Electrospinning conditions are: tip-to-collector distance = 10 cm and applied voltage = 15 kV.

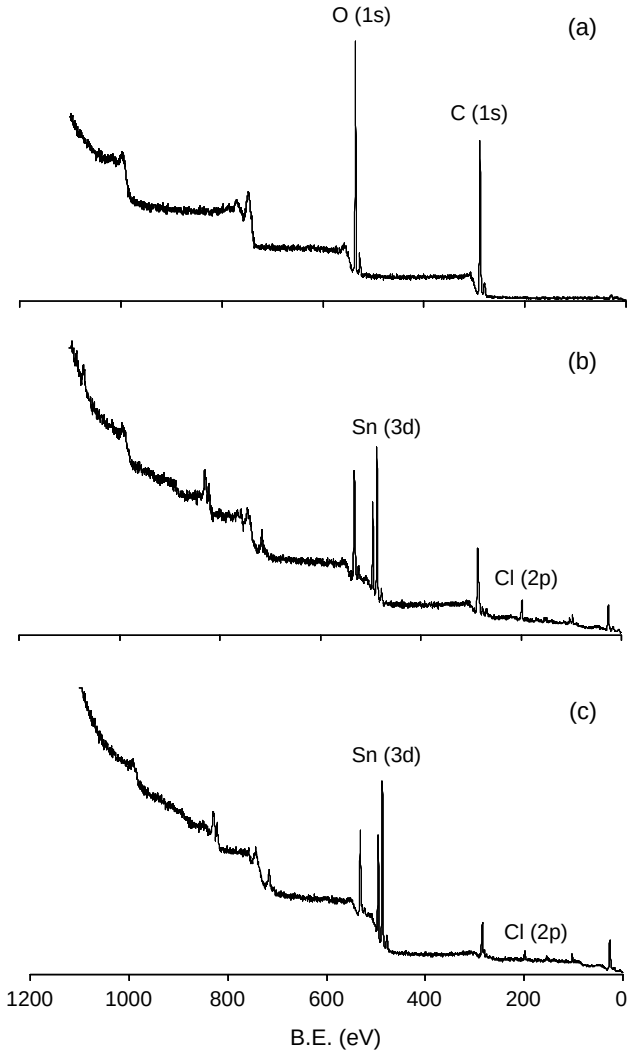

Fig. 14. Broad scan XPS analysis of HPC fibers without (a) and with (b) Sn^{2+} and Cl^{-} ions, and SnO_2 fibers deposited on the MEMS device (c). Electrospinning conditions are: tip-to-collector distance = 10 cm and applied voltage = 15 kV.

If the applied potential difference is increased further, multiple jets may be ejected from the Taylor cone [17,18]. As the jet travels from the base to the collector, its diameter decreases and the length increases in a way that keeps constant mass of charged polymer jet per unit time passing any point on the axis. The electric charges, in the form of ions, tend to drift in response to the applied electric field, and by doing so, they transfer the forces from the electric field to the polymer mass. As the electric charges move to the grounded terminal, they complete the electrical circuit, which provides the energy needed to accelerate the polymer.

Moreover, as the jet moves forward, the solvent may get evaporated depending on the surface tension of the polymer solution. This causes the jet diameter to decrease faster. As the jet diameter decreases with the simultaneous increase in its length, the electric charges are brought closer, and as a result, they start repelling each other, resulting in the bending instability of the fluid jet [11–16]. Simultaneously, the rapidly whipping jet produced via bending instability mechanism gets expanded in the radial direction and stretched along its axis, resulting in the deposition of thin charged polymer fibers on the grounded substrate. Under certain electrospinning conditions, upon the closest approach of the electric charges, the radial force becomes stronger than the cohesive strength of the charged polymer jet; and as a consequence, a single charged polymer jet splits into two or more jets (known as 'splaying' [1,19]), which along with the other mechanisms might occur alternatively during the operation of bending instability mechanism. This jet division may take place several times in rapid succession producing large number very fine electrically charged fibers moving towards collector. Since the deposited polymer fibers are charged, they repel the polymer fibers, which are deposited subsequently. Hence, the deposited polymer fibers do not overlap with each other but produce a highly porous mat of non-woven polymer fibers.

4.2. Bead formation characteristics of HPC polymer

In the present investigation, under certain electrospinning conditions, the HPC fibers are formed along with beads

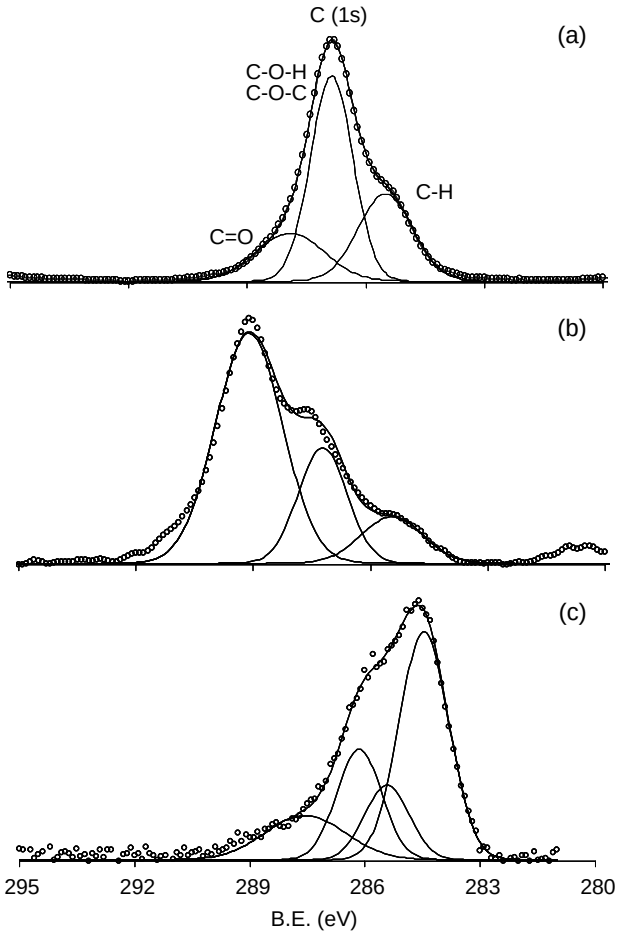

Fig. 15. Narrow scan XPS analysis of C(1s) spectrum for the HPC fibers without (a) and with (b) Sn^{2+} and Cl^{-} ions, and SnO_2 fibers deposited on the MEMS device (c). Electrospinning conditions are: tip-to-collector distance = 10 cm and applied voltage = 15 kV.

having a typical 'bead-on-string' morphology. Such bead formation has also been previously reported for various other polymer fibers obtained via electrospinning technique [3,19,20]. The formation of beads during the electrospinning of polymer fibers is a function of various processing parameters such as the solution viscosity, the surface tension, the applied voltage, the charge-concentration, the tip-to-collector distance, and the surrounding atmosphere (if the surface-charge is neutralized) [20]. The beads are basically formed during the electrospinning process if the forces such as viscoelastic, charge-repulsion, and electrostatic attraction, which tend to elongate the charged polymer jet are overcome by the surface tension force, which tend to break up and spherodize the charged polymer jet. The formation of beads, hence, suggests that under certain electrospinning conditions, the surface tension force on the charged polymer jet is not completely overcome by the combination of all counter forces.

It has been generally observed that, for obtaining the polymer fibers via electrospinning technique, there exists a viscosity range, above and below which the polymer solution

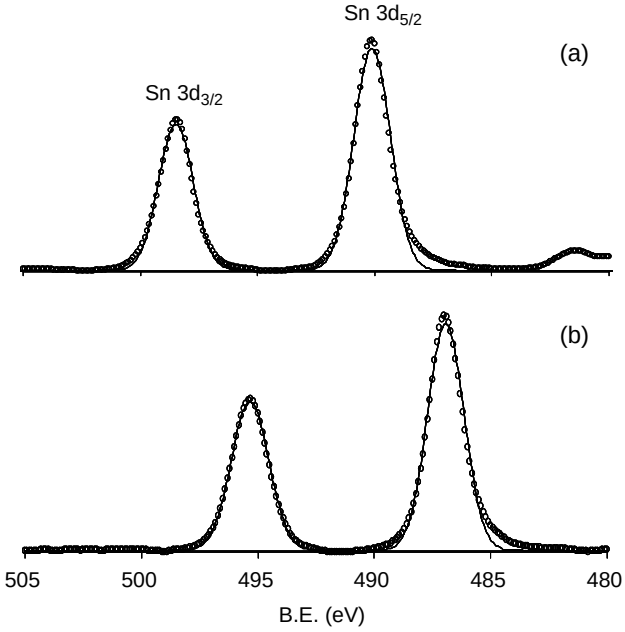

Fig. 16. Narrow scan XPS analysis of Sn(3d) for the HPC fibers with Sn^{2+} and Cl^{-} ions (a), and SnO_2 fibers (obtained after the calcination treatment) deposited on the MEMS device (b). Electrospinning conditions are: tip-to-collector distance = 10 cm and applied voltage = 15 kV.

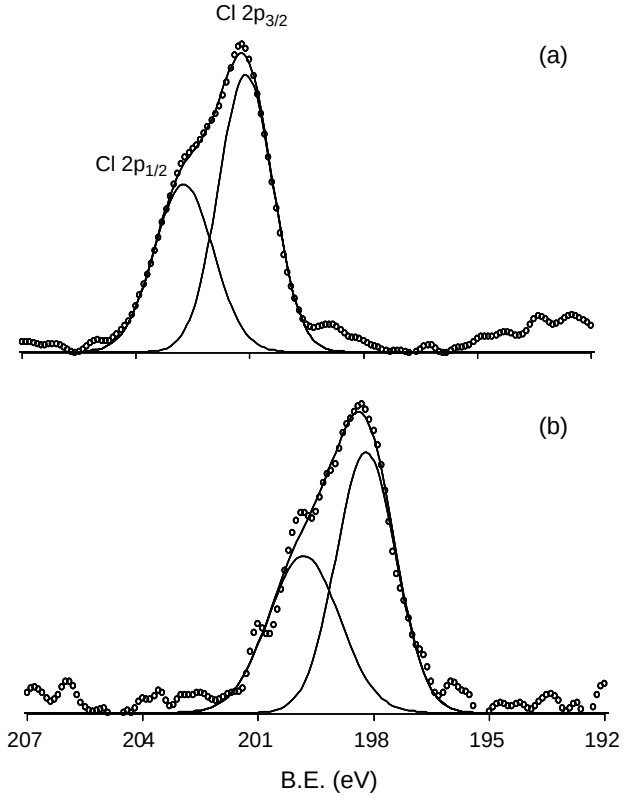

Fig. 17. Narrow scan XPS analysis of Cl(2p) for the HPC fibers with Sn^{2+} and Cl^{-} ions (a), and SnO_2 fibers (obtained after the calcination treatment) deposited on the MEMS device (b). Electrospinning conditions are: tip-to-collector distance = 10 cm and applied voltage = 15 kV.

cannot be electrospun [3]. This spinnable viscosity range is different for different polymers and may be different for the same polymer if the electrospinning conditions are varied. It is also reported that [3,21], at very low viscosity, within the spinnable viscosity range, only spherical particles (beads) are formed; while, at higher viscosity of the polymer solution, the polymer fibers are formed without any beads. For the intermediate viscosities, the polymer fibers are observed with beads. In the present investigation, since the HPC fibers are formed with beads (Figs. 2 and 5), the polymer concentration of 15 wt% possibly lies at the intermediate level within the spinnable concentration (or viscosity) range when ethanol is used as a solvent. In contrary, the HPC fibers are obtained without any beads when 2-propanol is used as solvent (Figs. 7 and 9). As a result, the polymer concentration of 15 wt% is possibly closer to the upper limit of the spinnable concentration (or viscosity) range when 2-propanol is used as solvent. It is clearly demonstrated here that, by using 2-propanol as a solvent instead of ethanol, the bead formation can be eliminated completely under the given electrospinning conditions. As far as the solvent-effect on the bead formation is concerned, the higher solution viscosity and lower surface tension of the polymer solution are reported to be the contributing factors [20]. Hence, it appears qualitatively that, these factors are more favorable in the case of 2-propanol than those in the case of ethanol since the HPC fibers with no beads are obtained using 2-propanol only.

We also note that, when ethanol is used as a solvent, more number of beads is formed as the applied potential difference is increased, which is in agreement with the earlier reports dealing with other polymers and other solvents [19,20]. In fact, increasing applied voltage should increase the total electric charge carried by the polymer jet, which in turn should reduce the bead formation tendency due to an enhanced elongation forces created by the mutual charge repulsion. This is, however, likely only if it is assumed that, the polymer fibers are formed with a single charged polymer jet with increasing applied voltage. In practice, however, multiple-jets are observed to be ejected from the Taylor cone with increasing applied potential difference [17]. Due to the multiple jet formation, the total surface-charge (that could have been carried by a single jet) gets distributed over number of jets, and as a result, the net surface-charge carried by each charged polymer jet becomes smaller. This reduced surface-charge should decrease the elongation force on each polymer jet, leading to the bead formation. Thus, the multiple jet formation is one of the primary factors contributing for increased bead number density with increasing applied potential difference. Secondly, the surface-charge carried by each individual charged polymer jet may also be further reduced by splaying as the charged polymer jet elongates and reduces its cross-section [1,19]. The reduced surface-charge as a result of splaying can further increase the bead number density. Hence, the increasing bead number density with increasing applied voltage, as observed in this investigation (Figs. 2 and 5), is attributed to the combined effect of multiple jet formation and splaying.

It is also observed that, the addition of Sn^{2+} and Cl^{-} ions to the HPC polymer solution drastically reduces the bead formation tendency (compare Figs. 2(b) and 11(a)). The addition of ions to the polymer solution has been suggested to increase the charge-concentration density within the polymer solution [20]. The increased elongation force on the charged polymer jet created by the enhanced charge repulsive and electrostatic attraction forces can effectively balance the surface tension force, giving rise to the formation of polymer fibers without any beads. As a result, although the HPC fibers with beads are formed, Fig. 2(b), under similar electrospinning conditions, the addition of Sn^{2+} and Cl^{-} ions to the HPC polymer solution could eliminate the beads, Fig. 11(a).

4.3. Nano and sub-micron fibers of HPC polymer

It is noted that, under almost all electrospinning conditions investigated here, the minimum HPC fiber diameter changes slightly with the applied voltage (Fig. 4). Moreover, for the HPC solution in both the solvents, the maximum HPC fiber diameter is observed to increase first with increasing applied potential difference, and then to decrease with further increase in the applied voltage above 20 or 25 kV depending on the electrospinning conditions. The trend in the variation in the average HPC fiber diameter is qualitatively observed to be similar to that in the maximum HPC fiber diameter as a function of the applied voltage. It has been suggested that [3,17], with increasing applied voltage, more charged polymer solution is ejected from the Taylor cone due to an increased charge-concentration within the polymer solution, which in turn increases the charged polymer jet diameter. Hence, the diameter of the polymer fiber deposited on the substrate is expected to increase with increasing applied voltage. In support of this, the maximum HPC fiber diameter is noted to increase initially with the applied voltage (Fig. 4). Moreover, the increased charge-concentration due to the addition of Sn^{2+} and Cl^{-} ions to the HPC solution, has also been observed to increase the maximum HPC fiber diameter from 400 to 720 nm under similar electrospinning conditions (compare Figs. 3(b) and 11(b)). At higher applied potential difference, however, the maximum HPC fiber diameter (and hence, possibly the average HPC fiber diameter) has been noted to decrease. This sudden decrease in the maximum fiber diameter at higher applied voltages is attributed here to the multiple jet formation [17] and the polymer jet splaying [1,19], under these electrospinning conditions. The formation of increased number of small diameter HPC fibers (Figs. 3 and 6) as well as the branched HPC fibers (Figs. 6(c) and 10(d)) are the evidences of the multiple jet formation and the polymer jet splaying processes occurring under these electrospinning conditions [19,22]. This is also in consonance with the bead formation and their increased number density with increasing applied voltage as discussed in the previous section.

Moreover, the inter fiber spacing has been qualitatively noted to increase with the applied voltage, and then, to decrease at higher applied potential differences (Figs. 3, 6, 8 and 10). This reduced inter fiber spacing at higher applied voltages also suggests that, the HPC fibers deposited under

these electrospinning conditions do not repel strongly due to the reduced surface-charge, which is a result of multiple jet formation and splaying at higher applied voltages. This further supports the decreased average HPC fiber diameter and increased bead number density as observed at higher applied potential differences.

It is also observed that, under similar ectrospinning conditions, the HPC fiber diameter is relatively much larger when 2-propanol, instead of ethanol, is used as a solvent (Fig. 4). In the previous section, due to the HPC fiber formation without the beads, it is deduced that, the HPC solution in 2-propanol possibly has higher solution viscosity and/or lower surface tension relative to that in ethanol. In the literature, it has been demonstrated that [17–20], both the increasing solution viscosity and decreasing surface tension result in increasing average polymer fiber diameter. Hence, the larger HPC fiber diameter observed with 2-propanol solvent has been qualitatively attributed here to the relatively higher solution viscosity and/or lower surface tension of the HPC solution in 2-propanol compared with that in ethanol.

4.4. HPC fibers assisted synthesis of semiconductor SnO_2 fibers

Nano and submicron fibers of various inorganic oxides, such as silica [23], germanium oxide [24], vanadium pentoxide [25], alumina-borate [26], and titania [27] have been derived using the electrospun polymer fibers as templates. In the present investigation, the synthesis of nano and submicron SnO_2 fibers, by using the HPC fibers as templates, has been demonstrated. The $SnCl_2$ precursor has been employed for this purpose and is mixed with the HPC solution in ethanol in a proper amount, which is selected on the basis of the concentration range used for other oxides, as demonstrated in the literature. As discussed earlier, the HPC fibers obtained with the addition of the Sn-precursor exhibit different electrospinning characteristics than those obtained without the addition of the Sn-precursor. Specifically, the HPC fibers are formed with small number of fine beads, increased average fiber diameter and inter fiber spacing, after the addition of Sn^{2+} and Cl^- ions (compare Fig. 2(b) with Fig. 11(a) and Fig. 3(b) with Fig. 11(b)). The calcination treatment at higher temperature results in complete burning of the HPC fibers (organic constituents) from the bulk fiber structure (compare Figs. 13(b) and (c)); however, the inorganic constituents still remain on the substrate (Fig. 13(c)), which are identified to be the nano and the submicron fibers (Fig. 12) of SnO_2 (Fig. 16(b)). The porous network of nano and submicron fibers of SnO_2, deposited on the MEMS device, short circuits the Au electrodes. It appears that, these SnO_2 fibers exhibit semiconductor behavior as suggested by the average electrical resistance of 450 Ω. Such micro-device is highly suitable for improving the detection time of inflammable gases, at lower operating temperatures, due to its porous structure [9].

It is necessary to mention that, the concentration of $SnCl_2$ precursor has not been varied in this investigation to study its effect on the final SnO_2 fiber diameter and its continuity, as well as on the initial diameter of the HPC-salt composite fiber. Work in this direction is in progress and the results of such study would be reported in the near future.

5. Conclusions

(1) Nano and submicron HPC fibers have been successfully synthesized, for the first time, via electrospinning technique. The characteristics of the electrospinning of HPC fibers are in accordance with those reported in the literature for other polymers and have been explained on the basis of the established mechanism associated with the electrospinning of polymer fibers.
(2) The HPC fibers synthesized in this investigation, are suited as templates for obtaining nano and submicron SnO_2 fibers. It has been demonstrated that, highly porous network of nano and submicron semiconductor SnO_2 fibers can be effectively deposited on the MEMS device for the gas sensing application by calcining the HPC fibers containing the Sn-precursor at higher temperature. The gas sensing tests for such micro-sensor are currently under investigation.

Acknowledgements

The authors thank UCF, Florida Space Grant Consortium (FSGC), NASA-Glenn (NASA NAG 32751), KSC-NASA, National Science Foundation (NSF EEC-0136710 and NSF CTS 0350572) (Seal) and NSF CAREER, ECS-0348603 (Cho) for funding the sensor and the nano-technology research.

References

[1] Reneker DH, Chun I. Nanotechnology 1996;7:216–23.
[2] Subbiah T, Bhat GS, Tock RW, Parameswaran S, Ramkumar SS. J Appl Polym Sci 2005;96:557–69.
[3] Huang Z-M, Zhang Y-Z, Kotaki M, Ramakrishna S. Compos Sci Technol 2003;63:2223–53.
[4] Doshi J, Reneker DH. J Electrostat 1995;35:151–60.
[5] Dersch R, Steinhart M, Boudriot U, Greiner A, Wendorff JH. Polym Adv Technol 2005;16:276–82.
[6] Li X, Liu H, Wang J, Cui H, Zhang X, Han F. Mater Sci Eng 2004;379:347–50.
[7] Shukla S, Seal S, Vanfleet R. J Sol–Gel Sci Technol 2003;27:119–36.
[8] Shukla S, Seal S, Vij R, Bandyopadhyay S. Nano Letts 2002;2:989–93.
[9] Shukla S, Agrawal R, Ludwig L, Cho HJ, Seal S. J Appl Phys 2005;97:054307–054319.
[10] Bar TL, Seal S. J Vac Sci Technol 1995;13:1239–46.
[11] Yarin AL, Koombhongse S, Reneker DH. J Appl Phys 2001;89:3018–26.
[12] Reneker DH, Yarin AL, Fong H, Koombhongse S. J Appl Phys 2000;87:4531–47.
[13] Yarin AL, Koombhongse S, Reneker DH. J Appl Phys 2001;90:4836–46.
[14] Shin YM, Hohman MM, Brenner MP, Rutledge GC. Appl Phys Lett 2001;78:1149–51.
[15] Hohman MM, Shin M, Rutledge G, Brenner MP. Phys Fluids 2001;13:2201–20.
[16] Shin YM, Hohman MM, Brenner MP, Rutledge GC. Polymer 2001;42:09955–09967.
[17] Demir MM, Yilgor I, Yilgor E, Erman B. Polymer 2002;43:3303–9.

[18] Theron SA, Yarin AL, Zussman E, Kroll E. Polymer 2005;46:2889–99.
[19] Deitzel JM, Kleinmeyer J, Harris D, Tan NCB. Polymer 2001;42:261–72.
[20] Fong H, Chun I, Reneker DH. Polymer 1999;40:4585–92.
[21] Lee KH, Kim HY, La YM, Lee DR, Sung NH. J Polym Sci, Part B: Polym Phys 2002;40:2259–68.
[22] Koombhonge S, Liu K, Reneker DH. J Polym Sci, Part B: Polym Phys 2001;39:2598–606.
[23] Choi S-S, Lee SG, Im SS, Kim SH. J Mater Sci Letts 2003;22:891–3.
[24] Kim HY, Viswanathmurthi P, Bhattarai N, Lee DR. Rev Adv Mater Sci 2003;5:220–3.
[25] Viswanathmurthi P, Bhattarai N, Kim HY, Lee DR. Scripta Mater 2003; 49:557–81.
[26] Dai H, Gong J, Kim H, Lee D. Nanotechnology 2002;13:674–7.
[27] Caruso RA, Schattka JH, Greiner A. Adv Mater 2001;13:1577–9.